Pressure in warm and hot dense matter using the average-atom model

Gérald Faussurier* and Christophe Blancard
CEA, DAM, DIF, F-91297 Arpajon, France

(Received 18 February 2019; published 3 May 2019)

Expressions of pressure in warm and hot dense matter using the average-atom model are presented. They are based on the stress-tensor approach. Nonrelativistic and relativistic cases are considered. The obtained formulas are simple and can be easily implemented in an average-atom model code. Comparisons with experimental data and quantum molecular dynamics and path integral Monte Carlo simulations are shown. The present formalism agrees well with experimental results for a large variety of elements in the warm dense matter regime and with *ab initio* simulations in the warm and hot dense matter regime for aluminum.

DOI: 10.1103/PhysRevE.99.053201

I. INTRODUCTION

The equation of state (EOS) is an essential physical ingredient for inertial confinement fusion (ICF) simulations [1,2]. An EOS model generally provides pressure and internal energy to close the hydrodynamics equations. Among the models that can be encountered, one distinguishes the *ab initio* approaches such as the path integral Monte Carlo (PIMC) [3] or quantum molecular dynamics (QMD) [4] methods. QMD can also be called density functional theory (DFT)-molecular dynamics (MD) [5]. Accurate data from these *ab initio* approaches have already been used in ICF simulations [6–9]. Not surprisingly, these simulations show the need for accurate EOS data to run the hydrodynamics codes.

QMD and PIMC have been shown to be complementary, with the QMD simulations being used in the warm dense matter regime and the PIMC simulations being used in the hot dense matter regime [10]. Yet, these two approaches are very time consuming, even on massively parallel supercomputers. Another possibility to calculate EOS data is to consider the full-quantum average-atom model (AAM) in a muffin-tin approximation [11–20]. Such a model is very fast compared to PIMC or QMD simulations and is very helpful in building data tables for hydrodynamics simulations. It has been shown that the average-atom model is consistent with the QMD and PIMC simulations [21].

Nevertheless, among the methods that can be used to calculate the pressure, i.e., from the free energy, the virial theorem, or the stress-tensor methods, there is no general agreement and the consistency between them is often obscure. This is the case both in the nonrelativistic and relativistic formalisms.

In this paper, we consider the calculation of pressure from the stress tensor. Formulas already exist for spherical potentials which are well suited for the AAM. These formulas have been first deduced from a nonrelativistic formalism [22], then using a semirelativistic approach [15], and recently expressed in a relativistic formulation [23]. However, in all these works, the pressure is evaluated using the radial component of the stress tensor, an approach for which More [22] warned that "there is no formal justification for this assumption." To go beyond this approximation, we propose an expression to calculate the pressure which is consistent with the formula derived by Johnson [24] from the stress tensor and angular algebra. In a first part, we give the expressions of pressure for the bound and the free electrons. We use the stress tensor to derive the relativistic extension of these formulas. We show the consistency between the nonrelativistic and relativistic expressions and with the free-electron gas. In a second part we compare the present AAM calculation of pressure with experiment and with DFT-MD/PIMC simulations. The last part is the conclusion. In the Appendix, we give useful formulas for the spherical Bessel functions of the first kind that are needed to show the consistency between the AAM model and the free-electron gas.

II. THEORY

A. Nonrelativistic case

In his article [22], More gives an expression to calculate the electronic pressure in hot dense matter starting from the stress tensor [25]. Unfortunately, the expression suffers from being poorly justified from first principles although it is consistent, as we shall see, with the nonrelativistic free-electron pressure

$$P_f^{\mathrm{nr}} = \frac{2\sqrt{2}m_e^{3/2}(k_BT)^{5/2}}{3\pi^2\hbar^3} I_{3/2}(\eta), \tag{1}$$

where m_e is the electron mass, k_B the Boltzmann constant, $\hbar$ the reduced Planck constant, and T the temperature. Here, $\eta = \mu/k_BT$, where μ is the chemical potential. $I_{3/2}(\eta)$ is the Fermi-Dirac integral of order 3/2 [26,27], i.e.,

$$I_n(\eta) = \int_0^{+\infty} dx \frac{x^n}{1+e^{x-\eta}}. \tag{2}$$

More gives the expression of the stress tensor in spherical coordinates. Considering only the continuum electrons, we

*Corresponding author: gerald.faussurier@cea.fr

have for the radial part [22]

$$T_{rr} = \frac{\hbar^2}{2m_e}\sum_\ell \frac{2(2\ell+1)}{4\pi}\int_0^{+\infty} d\varepsilon f(\varepsilon) \left[\left(\frac{d}{dr}\frac{P_{\varepsilon\ell}(r)}{r}\right)^2 - \frac{P_{\varepsilon\ell}(r)}{r}\frac{d^2}{dr^2}\left(\frac{P_{\varepsilon\ell}(r)}{r}\right)\right]_R, \quad (3)$$

where

$$f(\varepsilon) = \frac{1}{1+e^{\varepsilon/k_BT-\eta}}, \quad (4)$$

ℓ is the orbital quantum number, and

$$\varepsilon = \frac{\hbar^2 k^2}{2m_e} \quad (5)$$

is the energy. k is the angular wave number. The subscript R means that the calculation of the quantity inside the brackets is done at radius $r = R$. More proposed to calculate the pressure P from the equation $P = T_{rr}$. We consider the continuum eigenfunctions

$$\psi_s = (1/r)P_{\varepsilon\ell}(r)Y_\ell^m(\theta,\phi)\chi_\sigma \quad (6)$$

that satisfy the self-consistent Schrödinger equation

$$-\frac{\hbar^2}{2m_e}\Delta\psi_s + V(r)\psi_s = \varepsilon_s\psi_s. \quad (7)$$

m is the magnetic quantum number [28] and s is a generic quantum number. The self-consistent field potential $V(r)$ is such that $V(r) = 0$ when $r \geqslant R$. R is the Wigner-Seitz radius with $4\pi R^3 N_i/3 = 1$, where N_i is the ion density. $V(r)$ is calculated in the average-atom model [29]. It contains [30] the electrostatic interaction of the electrons with the nucleus, the electrostatic interaction between the electrons, and the exchange-correlation potential [31]. $Y_\ell^m(\theta,\phi)$ is a spherical harmonics and χ_σ a two-component electron spinor. For bound eigenfunctions, we have

$$\psi_s = (1/r)P_{n\ell}(r)Y_\ell^m(\theta,\phi)\chi_\sigma. \quad (8)$$

n is the principal quantum number. The bound eigenfunctions (8) satisfy also the self-consistent Schrödinger equation (7). The continuum eigenfunctions are normalized such that

$$\int_0^{+\infty} dr P_{\varepsilon\ell}(r)P_{\varepsilon'\ell}(r) = \delta(\varepsilon-\varepsilon'), \quad (9)$$

whereas for the bound eigenfunctions we have

$$\int_0^{+\infty} dr P_{n\ell}(r)P_{n'\ell}(r) = \delta_{nn'}. \quad (10)$$

In Eq. (3), the index $_R$ means that we calculate the expression of interest in R, i.e., at the surface of the average-atom sphere. The chemical potential μ is determined such that

$$\int_0^R 4\pi r^2[n_b(r)+n_f(r)]dr = Z, \quad (11)$$

where $n_b(r)$ and $n_f(r)$ are the bound- and free-electron densities of the average atom. Z is the nuclear charge. We assume that the ion and electron temperatures are equal. The total electron density of the average atom $n(r) = n_b(r) + n_f(r)$, where

$$4\pi r^2 n_b(r) = \sum_{n\ell}\frac{2(2\ell+1)}{1+e^{(\varepsilon_{n\ell}-\mu)/k_BT}}P_{n\ell}(r)^2 \quad (12)$$

and

$$4\pi r^2 n_f(r) = \sum_\ell \int_0^{+\infty} d\varepsilon \frac{2(2\ell+1)}{1+e^{(\varepsilon-\mu)/k_BT}}P_{\varepsilon\ell}(r)^2. \quad (13)$$

Let us find another expression for T_{rr} in Eq. (3) using the Schrödinger equation with $V(R) = 0$. We have also [22,28]

$$T_{rr} = \frac{\hbar^2}{2m_e}\sum_\ell \frac{2(2\ell+1)}{4\pi R^2}\int_0^{+\infty} d\varepsilon f(\varepsilon)\left[\left(\frac{dP_{\varepsilon\ell}(r)}{dr}\right)^2 + \left(k^2 - \frac{\ell^2+\ell+1}{r^2}\right)P_{\varepsilon\ell}(r)^2\right]_R. \quad (14)$$

Since the stress tensor is diagonal, for the last diagonal components we find that [22]

$$T_{\theta\theta} = T_{\phi\phi} = \frac{\hbar^2}{2m_e}\sum_\ell \frac{2(2\ell+1)}{4\pi R^2}\int_0^{+\infty} d\varepsilon f(\varepsilon)\left[\frac{\ell^2+\ell+1}{r^2}P_{\varepsilon\ell}(r)^2 - \frac{1}{2r}\frac{d}{dr}P_{\varepsilon\ell}(r)^2\right]_R. \quad (15)$$

The radial eigenfunctions can be chosen to be real. Instead of calculating the pressure P such that $P = T_{rr}$, we propose to calculate P taking one-third of the trace of T, i.e.,

$$P = \frac{1}{3}(T_{rr} + T_{\theta\theta} + T_{\phi\phi}). \quad (16)$$

We thus find that

$$P_{\text{contin}}^{\text{nr}} = \frac{\hbar^2}{24\pi m_e}\int_0^{+\infty} d\varepsilon f(\varepsilon)\sum_\ell 2(2\ell+1)\left\{\left[\frac{d}{dr}\left(\frac{P_{\varepsilon\ell}(r)}{r}\right)\right]^2 + k^2\left(\frac{P_{\varepsilon\ell}(r)}{r}\right)^2 + \frac{\ell(\ell+1)}{r^2}\left(\frac{P_{\varepsilon\ell}(r)}{r}\right)^2\right\}_R. \quad (17)$$

This expression is consistent with the one derived by Johnson [24] using the stress-tensor approach and angular algebra. $P_{\text{contin}}^{\text{nr}}$ is clearly positive. For bound electrons, we find that

$$P_{\text{bound}}^{\text{nr}} = \frac{\hbar^2}{24\pi m_e}\sum_{n\ell} 2(2\ell+1)f(\varepsilon_{n\ell})\left\{\left[\frac{d}{dr}\left(\frac{P_{n\ell}(r)}{r}\right)\right]^2 + \frac{2m_e}{\hbar^2}\varepsilon_{n\ell}\left(\frac{P_{n\ell}(r)}{r}\right)^2 + \frac{\ell(\ell+1)}{r^2}\left(\frac{P_{n\ell}(r)}{r}\right)^2\right\}_R. \quad (18)$$

Because $\varepsilon_{n\ell}$ takes negative values, $P^{\rm nr}_{\rm bound}$ has no definite sign. Moreover, there is no additional component such as the one coming from the exchange and correlations [24]. Exchange and correlation effects are taken into account in the self-consistent field potential $V(r)$, and so in the bound and free eigenfunctions.

Let us now show that Eq. (17) is consistent with the nonrelativistic free-electron gas pressure $P^{\rm nr}_f$ given by Eq. (1). For the free case, we have $V(r) = 0$ and

$$P^0_{\varepsilon\ell}(r) = \sqrt{\frac{2m_e}{\hbar^2\pi k}}\, kr\, j_\ell(kr). \tag{19}$$

Introducing the variable $z = kr$, we find that

$$P = \frac{1}{12\pi^2}\int_0^{+\infty} d\varepsilon f(\varepsilon)k^3 \sum_\ell 2(2\ell+1)\left\{\left[\frac{dj_\ell(z)}{dz}\right]^2 + \frac{\ell(\ell+1)}{z^2}j_\ell^2(z) + j_\ell^2(z)\right\}_R. \tag{20}$$

Using Eqs. (A5) and (5), we recover the pressure of the nonrelativistic free-electron pressure (1).

We can do the same thing for the components of the stress tensor T_{rr} and $T_{\theta\theta}$. Let us start with T_{rr} given by Eq. (3). Using Eqs. (5), (19), (A4), and (A6), we find that $T_{rr} = P^{\rm nr}_f$. As for $T_{\theta\theta}$ given by Eq. (15), using Eqs. (5), (19), (A3), and (A10), we also find that $T_{\theta\theta} = P^{\rm nr}_f$. We can see that the each component of the stress tensor expressed in spherical coordinates is equal to the pressure of the nonrelativistic free-electron pressure in the free-electron gas case.

B. Relativistic case

We derive the relativistic pressure for one electron in the self-consistent field potential $V(r)$ assuming that $V(r) = 0$ when $r \geqslant R$ and using the stress-tensor approach [24]. This assumption is essential for what follows. The time-dependent Dirac equation for one electron in the potential $V(r)$ reads

$$i\hbar\frac{\partial\psi}{\partial t} = [c\vec{\alpha}\cdot\mathbf{p} + \beta m_e c^2 + V]\psi. \tag{21}$$

Here, ψ is a four-dimensional bispinor and c the speed of light. $\vec{\alpha}$ and β are the Dirac matrices. We have explicitly

$$\vec{\alpha} = \begin{pmatrix} 0 & \vec{\sigma} \\ \vec{\sigma} & 0 \end{pmatrix} \tag{22}$$

and

$$\beta = \begin{pmatrix} \mathbb{1}_2 & 0 \\ 0 & -\mathbb{1}_2 \end{pmatrix}. \tag{23}$$

$\vec{\sigma}$ are the Pauli matrices, i.e.,

$$\sigma_1 = \sigma_x = \begin{pmatrix} 0 & 1 \\ 1 & 0 \end{pmatrix}, \tag{24}$$

$$\sigma_2 = \sigma_y = \begin{pmatrix} 0 & -i \\ i & 0 \end{pmatrix}, \tag{25}$$

and

$$\sigma_3 = \sigma_z = \begin{pmatrix} 1 & 0 \\ 0 & -1 \end{pmatrix}. \tag{26}$$

Moreover,

$$\mathbb{1}_2 = \begin{pmatrix} 1 & 0 \\ 0 & 1 \end{pmatrix}. \tag{27}$$

So,

$$i\hbar\frac{\partial\psi}{\partial t} = -i\hbar c\alpha_i\partial_i\psi + m_e c^2\beta\psi + V\psi. \tag{28}$$

Taking the complex conjugate of this expression and remembering that the matrices α_i and β are Hermitian, we have

$$-i\hbar\frac{\partial\psi^\dagger}{\partial t} = i\hbar c\partial_i\psi^\dagger\alpha_i + m_e c^2\psi^\dagger\beta + \psi^\dagger V. \tag{29}$$

The dagger means Hermitian conjugation. We can now calculate the rate of increase of the ith component of the electron momentum inside the Wigner-Seitz cell. Since

$$\langle p_i\rangle = \int_R d\tau\,\psi^\dagger p_i\psi, \tag{30}$$

we have

$$\frac{d}{dt}\langle p_i\rangle = \int_R d\tau\left(\frac{\partial\psi^\dagger}{\partial t}p_i\psi + \psi^\dagger p_i\frac{\partial\psi}{\partial t}\right). \tag{31}$$

So, using Eqs. (28) and (29), we find that

$$\frac{d}{dt}\langle p_i\rangle = -\int_R d\tau\,\partial_j[c\psi^\dagger\alpha_j p_i\psi] - \int_R d\tau\,\psi^\dagger\partial_i V\psi. \tag{32}$$

We can introduce the relativistic stress tensor

$$T_{ji} = c\psi^\dagger\alpha_j p_i\psi \tag{33}$$

and the pressure by taking one-third of the trace of this stress tensor [29], i.e.,

$$P = \frac{1}{3}c\psi^\dagger\vec{\alpha}\cdot\mathbf{p}\psi. \tag{34}$$

This result generalizes the nonrelativistic expression [24]

$$P = \frac{\hbar^2}{6m_e}(\vec{\nabla}\psi^\dagger\cdot\vec{\nabla}\psi - \psi^\dagger\Delta\psi). \tag{35}$$

Taking nonrelativistic plane waves for ψ, i.e., $\psi(\mathbf{r}) = (1/\sqrt{\mathcal{V}})e^{i\mathbf{p}\cdot\mathbf{r}/\hbar}$, one can check that we recover the nonrelativistic free-electron gas pressure (1) starting from

$$P = \frac{\hbar^2}{6m_e}\sum_{\mathbf{k},s} f(\varepsilon_{\mathbf{k}})(\vec{\nabla}\psi^\dagger\cdot\vec{\nabla}\psi - \psi^\dagger\Delta\psi), \tag{36}$$

where $\varepsilon_{\mathbf{k}}$ is given by (5) and $\mathcal{V}$ is the volume of the system [24].

We can do the same thing in the relativistic case starting from

$$P = \frac{1}{3}\sum_{\mathbf{k},s} f(\varepsilon_{\mathbf{k}}) c\psi_s^\dagger \vec{\alpha}\cdot\mathbf{p}\psi_s, \tag{37}$$

where [32]

$$\psi_s(\mathbf{r}) = \frac{1}{\sqrt{\mathcal{V}}} e^{i\mathbf{p}\cdot\mathbf{r}/\hbar}\sqrt{\frac{E_p + m_e c^2}{2E_p}} U(p,s). \tag{38}$$

$U(p,s)$ is a bispinor [33], i.e.,

$$U(p,s) = \begin{pmatrix} \chi_s \\ \frac{c\vec{\sigma}\cdot\mathbf{p}}{E_p + m_e c^2}\chi_s \end{pmatrix}. \tag{39}$$

χ_s with $s = 1, 2$ are the spinors defined by

$$\chi_1 = \begin{pmatrix} 1 \\ 0 \end{pmatrix} \tag{40}$$

and

$$\chi_2 = \begin{pmatrix} 0 \\ 1 \end{pmatrix}. \tag{41}$$

$\sqrt{\frac{E_p+m_e c^2}{2E_p}}$ is a normalization factor such that [33]

$$\sqrt{\frac{E_p + m_e c^2}{2E_p}} U^\dagger(p,s)\sqrt{\frac{E_p + m_e c^2}{2E_p}} U(p,s) = 1. \tag{42}$$

$\psi_s(\mathbf{r})$ is a solution of the Dirac equation [32]

$$E_p\psi_s(\mathbf{r}) = (c\vec{\alpha}\cdot\mathbf{p} + \beta m_e c^2)\psi_s(\mathbf{r}), \tag{43}$$

where $E_p = \sqrt{p^2c^2 + m_e^2c^4}$ and $\varepsilon_{\mathbf{k}} = \sqrt{\hbar^2c^2k^2 + m_e^2c^4} - m_e c^2$. Using the operator identity satisfied by the Pauli matrices [32], i.e.,

$$(\vec{\sigma}\cdot\mathbf{v})(\vec{\sigma}\cdot\mathbf{w}) = (\mathbf{v}.\mathbf{w})\mathbb{1}_2 + i\vec{\sigma}\cdot(\mathbf{v}\times\mathbf{w}), \tag{44}$$

where $\mathbf{v}$ and $\mathbf{w}$ are vectors in three dimensions, we find that P is equal to

$$P_f^{\rm rel} = \frac{2^{3/2}m_e^4c^5\theta^{5/2}}{3\pi^2\hbar^3}\left[F_{3/2}(\eta,\theta) + \frac{\theta}{2}F_{5/2}(\eta,\theta)\right], \tag{45}$$

where $P_f^{\rm rel}$ is the relativistic free-electron gas pressure [34],

$$F_k(\eta,\theta) = \int_0^{+\infty} dx \frac{x^k\sqrt{1 + \frac{\theta x}{2}}}{1 + e^{x-\eta}} \tag{46}$$

is the generalized Fermi-Dirac integral [35,36], and $\theta = k_B T/m_e c^2$.

It is interesting to propose another way to calculate the pressure. Since the wave functions (38) satisfy the Dirac equation (43), one can also calculate the pressure as follows, i.e.,

$$P = \frac{1}{3}\sum_{\mathbf{k},s} f(\varepsilon_{\mathbf{k}})\psi_s^\dagger(E_p - m_e c^2\beta)\psi_s. \tag{47}$$

This way of calculating the pressure can be used in the general case to avoid the difficulty of calculating $\psi^\dagger c\vec{\alpha}\cdot\mathbf{p}\psi$ with eigenfunctions associated with a spherical self-consistent field potential $V(r)$. The trick will work since we calculate the pressure at the surface of the average-atom sphere for which $V(R) = 0$. So, for bound states [37],

$$P = \frac{1}{3}\sum_{n,\kappa,m} f(\varepsilon_{n\kappa})\left[\psi_{n\kappa m}^\dagger(E_{n\kappa} - \beta m_e c^2)\psi_{n\kappa m}\right]_R, \tag{48}$$

where [37]

$$\psi_{\kappa m} = \frac{1}{r}\begin{pmatrix} iP_{n\kappa}(r)\Omega_{\kappa m}(\theta,\phi) \\ Q_{n\kappa}(r)\Omega_{-\kappa m}(\theta,\phi) \end{pmatrix}. \tag{49}$$

$\Omega_{\kappa m}$ is a spherical spinor, $P_{n\kappa}(r)$ is the large component, and $Q_{n\kappa}(r)$ the small component. Using the identity [38]

$$\sum_m \Omega_{\kappa m}^\dagger(\theta,\phi)\Omega_{\kappa m}(\theta,\phi) = \sum_m \Omega_{-\kappa m}^\dagger(\theta,\phi)\Omega_{-\kappa m}(\theta,\phi) = \frac{2|\kappa|}{4\pi} \tag{50}$$

and knowing that [39] $2j + 1 = 2|\kappa|$, we find that

$$P_{\rm bound}^{\rm rel} = \frac{1}{3}\sum_{n,\kappa}\frac{2|\kappa|}{4\pi R^2} f(\varepsilon_{n\kappa})\left[(E_{n\kappa} - m_e c^2)P_{n\kappa}^2(r) + (E_{n\kappa} + m_e c^2)Q_{n\kappa}^2(r)\right]_R, \tag{51}$$

since the radial wave functions can be chosen to be real [37]. For continuum electrons, we find that

$$P_{\rm contin}^{\rm rel} = \frac{1}{3}\int_0^{+\infty} d\varepsilon \sum_\kappa \frac{2|\kappa|}{4\pi R^2} f(\varepsilon)\left[(E_p - m_e c^2)P_{\varepsilon\kappa}^2(r) + (E_p + m_e c^2)Q_{\varepsilon\kappa}^2(r)\right]_R. \tag{52}$$

The relativistic average-atom model equations in a muffin-tin approximation read [37,40]

$$\begin{aligned} [V(r) + m_e c^2]P_a(r) + \hbar c\left[\tfrac{dQ_a(r)}{dr} - \tfrac{\kappa_a}{r}Q_a(r)\right] &= E_a P_a(r), \\ -\hbar c\left[\tfrac{dP_a(r)}{dr} + \tfrac{\kappa_a}{r}P_a(r)\right] + [V(r) - m_e c^2]Q_a(r) &= E_a Q_a(r), \end{aligned} \tag{53}$$

where $V(r)$ is the spherical self-consistent potential that is calculated as in the nonrelativistic case. $a = (n,\kappa)$ for bound states and $a = (\varepsilon,\kappa)$ for continuum states. The spherical spinors satisfy the orthogonality relations

$$\int_0^\pi \sin(\theta)d\theta\int_0^{2\pi} d\phi\,\Omega_{\kappa' m'}^\dagger(\theta,\phi)\Omega_{\kappa m}(\theta,\phi) = \delta_{\kappa\kappa'}\delta_{mm'}. \tag{54}$$

As for the bound large and small components, we have the orthogonality relations [41]

$$\int_0^{+\infty} dr[P_{n\kappa}(r)P_{n'\kappa}(r) + Q_{n\kappa}(r)Q_{n'\kappa}(r)] = \delta_{nn'}. \quad (55)$$

Concerning the free large and small components, we have

$$\int_0^{+\infty} dr[P_{\varepsilon\kappa}(r)P_{\varepsilon'\kappa}(r) + Q_{\varepsilon\kappa}(r)Q_{\varepsilon'\kappa}(r)] = \delta(\varepsilon - \varepsilon'). \quad (56)$$

The electron density $n(r)$ is the sum of the bound $n_b(r)$ and the free $n_f(r)$ electron densities. They read

$$4\pi r^2 n_b(r) = \sum_a \frac{2|\kappa_a|}{1 + e^{\varepsilon_a/k_BT - \eta}}\left[P_a^2(r) + Q_a^2(r)\right] \quad (57)$$

and

$$4\pi r^2 n_f(r) = \int_0^{+\infty} d\varepsilon \sum_\kappa \frac{2|\kappa|}{1 + e^{\varepsilon/k_BT - \eta}}\left[P_{\varepsilon\kappa}^2(r) + Q_{\varepsilon\kappa}^2(r)\right]. \quad (58)$$

As in the nonrelativistic case, the chemical potential μ is determined such that Eq. (11) is satisfied. ε_a, ε, and μ do not contain the rest-mass energy.

Let us check the consistency of $P_{\text{contin}}^{\text{rel}}$ with the relativistic free-electron gas P_f^{rel}. When $V(r) = 0$, we know that [24]

$$P_{\varepsilon\kappa}^0(r) = kr\, j_{\ell(\kappa)}(kr)\sqrt{\frac{E_p + m_ec^2}{\hbar^2\pi c^2 k}} \quad (59)$$

and

$$Q_{\varepsilon\kappa}^0(r) = -\text{sgn}(\kappa)kr\, j_{\ell(-\kappa)}(kr)\sqrt{\frac{E_p - m_ec^2}{\hbar^2\pi c^2 k}}, \quad (60)$$

where $\text{sgn}(\kappa)$ is the sign of κ. Using the identities

$$\sum_\kappa |\kappa| j_{\ell(\kappa)}^2(kr) = \sum_\kappa |\kappa| j_{\ell(-\kappa)}^2(kr) = 1, \quad (61)$$

we find that $P_{\text{contin}}^{\text{rel}}$ is equal to P_f^{rel} in the free-electron gas case.

Let us now study the nonrelativistic limit of (51) and (52). Let us begin with the continuum electrons. From Eq. (53), we know that

$$[m_ec^2 + V(r)]P_{\varepsilon\kappa}(r) + \hbar c\left[\frac{dQ_{\varepsilon\kappa}(r)}{dr} - \frac{\kappa}{r}Q_{\varepsilon\kappa}(r)\right] = E_pP_{\varepsilon\kappa}(r) \quad (62)$$

and

$$-\hbar c\left[\frac{dP_{\varepsilon\kappa}(r)}{dr} + \frac{\kappa}{r}P_{\varepsilon\kappa}(r)\right] + [V(r) - m_ec^2]Q_{\varepsilon\kappa}(r) = E_pQ_{\varepsilon\kappa}(r). \quad (63)$$

So, remembering that $V(r) = 0$ for $r \geqslant R$, we have

$$(E_p - m_ec^2)P_{\varepsilon\kappa}(r) = \hbar c\left[\frac{dQ_{\varepsilon\kappa}(r)}{dr} - \frac{\kappa}{r}Q_{\varepsilon\kappa}(r)\right] \quad (64)$$

and

$$(E_p + m_ec^2)Q_{\varepsilon\kappa}(r) = -\hbar c\left[\frac{dP_{\varepsilon\kappa}(r)}{dr} + \frac{\kappa}{r}P_{\varepsilon\kappa}(r)\right], \quad (65)$$

or, in the nonrelativistic regime, $E_p + m_ec^2 \approx 2m_ec^2$, and $E_p - m_ec^2 \approx \frac{\hbar^2k^2}{2m_e}$. We find that

$$P_{\text{contin}}^{\text{rel}} \approx \frac{\hbar^2}{6m_e}\int_0^{+\infty} d\varepsilon f(\varepsilon)\sum_\kappa \frac{2|\kappa|}{4\pi R^2}\left[k^2P_{\varepsilon\kappa}(r)^2 + \left(\frac{dP_{\varepsilon\kappa}(r)}{dr}\right)^2 + \frac{2\kappa}{r}\frac{dP_{\varepsilon\kappa}(r)}{dr}P_{\varepsilon\kappa}(r) + \frac{\kappa^2}{r^2}P_{\varepsilon\kappa}^2(r)\right]_R. \quad (66)$$

We now examine the various terms involved in the summation on κ. We remember that $\kappa = -\ell - 1$ for $j = \ell + 1/2$ and $\kappa = \ell$ for $j = \ell - 1/2$. So,

$$\sum_\kappa |\kappa|\kappa\frac{dP_{\varepsilon\kappa}(r)}{dr}P_{\varepsilon\kappa}(r) \approx -\sum_{\ell=0}^{+\infty}(2\ell + 1)\frac{dP_{\varepsilon\ell}(r)}{dr}P_{\varepsilon\ell}(r). \quad (67)$$

Next,

$$\sum_\kappa |\kappa|P_{\varepsilon\kappa}(r)^2 \approx \sum_{\ell=0}^{+\infty}(2\ell + 1)P_{\varepsilon\ell}^2(r). \quad (68)$$

In the same spirit,

$$\sum_\kappa |\kappa|\left(\frac{dP_{\varepsilon\kappa}(r)}{dr}\right)^2 \approx \sum_{\ell=0}^{+\infty}(2\ell + 1)\left(\frac{dP_{\varepsilon\ell}(r)}{dr}\right)^2. \quad (69)$$

Finally,

$$\sum_{\kappa}|\kappa|\kappa^2 P_{\varepsilon\kappa}^2(r)\approx\sum_{\ell=0}^{+\infty}\ell(\ell+1)(2\ell+1)P_{\varepsilon\ell}^2(r)+\sum_{\ell=0}^{+\infty}(2\ell+1)P_{\varepsilon\ell}^2(r). \tag{70}$$

We now insert Eqs. (67)–(70) inside Eq. (66). We obtain Eq. (17), where we identify the large component with the nonrelativistic free wave function. Let us consider the bound electrons. The derivation is very similar. Since $E_{n\kappa}-m_ec^2=\varepsilon_{n\kappa}$ and $E_{n\kappa}+m_ec^2\approx 2m_ec^2$, we have

$$2m_ec^2Q_{n\kappa}(r)\approx-\hbar c\left[\frac{dP_{n\kappa}(r)}{dr}+\frac{\kappa}{r}P_{n\kappa}(r)\right]. \tag{71}$$

Starting from Eq. (51), we find that

$$P_{\text{bound}}^{\text{rel}}\approx\frac{\hbar^2}{6m_e}\sum_{n,\kappa}\frac{2|\kappa|}{4\pi R^2}f(\varepsilon_{n\kappa})\left[\frac{2m_e}{\hbar^2}\varepsilon_{n\kappa}P_{n\kappa}^2(r)+\left(\frac{dP_{n\kappa}(r)}{dr}\right)^2+\frac{2\kappa}{r}\frac{dP_{n\kappa}(r)}{dr}P_{n\kappa}(r)+\frac{\kappa^2}{r^2}P_{n\kappa}^2(r)\right]_R. \tag{72}$$

We proceed as above by calculating the various sums in κ in the nonrelativistic approximation. We thus have

$$\sum_{\kappa}f(\varepsilon_{n\kappa})|\kappa|\kappa\frac{dP_{n\kappa}(r)}{dr}P_{n\kappa}(r)\approx-\sum_{\ell=0}^{+\infty}f(\varepsilon_{n\ell})(2\ell+1)\frac{dP_{n\ell}(r)}{dr}P_{n\ell}(r), \tag{73}$$

$$\sum_{\kappa}f(\varepsilon_{n\kappa})|\kappa|\varepsilon_{n\kappa}P_{n\kappa}^2(r)\approx\sum_{\ell=0}^{+\infty}f(\varepsilon_{n\ell})(2\ell+1)\varepsilon_{n\ell}P_{n\ell}^2(r), \tag{74}$$

$$\sum_{\kappa}f(\varepsilon_{n\kappa})|\kappa|\left(\frac{dP_{n\kappa}(r)}{dr}\right)^2\approx\sum_{\ell=0}^{+\infty}f(\varepsilon_{n\ell})(2\ell+1)\left(\frac{dP_{n\ell}(r)}{dr}\right)^2, \tag{75}$$

and

$$\sum_{\kappa}f(\varepsilon_{n\kappa})|\kappa|\kappa^2P_{n\kappa}^2(r)\approx\sum_{\ell=0}^{+\infty}f(\varepsilon_{n\ell})\ell(\ell+1)(2\ell+1)P_{n\ell}^2(r)+\sum_{\ell=0}^{+\infty}f(\varepsilon_{n\ell})(2\ell+1)P_{n\ell}^2(r). \tag{76}$$

Inserting Eqs. (73)–(76) inside Eq. (72), we obtain Eq. (18).

In summary, we have verified that the relativistic expressions of the pressure for the bound and continuum electrons are consistent with the nonrelativistic expressions.

III. NUMERICAL APPLICATIONS

We compare in Figs. 1 and 2 the pressure calculated using Eqs. (17) and (18) for AAM to QMD simulations and experimental results obtained from the isochoric closed vessel plasma (EPI for Enceinte à Plasma Isochore) [42]. We add ion ideal perfect gas (PG) pressure to the electronic pressure in the AAM approach to obtain the total pressure. We can see that the AAM calculations are consistent with PG at low temperature. This can be understood because below 10 000 K, we have a dilute gas of nearly neutral atoms. The average ionization is small and the pressure is readily given by PG since the interaction between quasineutral atoms is small compared to PG. Note that experimental results are below PG for Si, Al, Ag, and Cu. When the temperature increases, AAM departs from PG due to the increase of ionization. What is striking is the good agreement between QMD and AAM for all the cases presented above 15 000 K. Note that PG and AAM fall above both QMD and experiment data points at low temperature. Similar trends are valid for Al at 0.1 g/cm^3 and Cu at 0.3 g/cm^3 (not shown here). The bound component to the pressure is negligible compared to the continuum component. In the present regime, the continuum electrons form a nearly ideal free nondegenerate gas. We could imagine how to calculate the total pressure by $\bar{Z}+1$ times PG. The problem is to determine the average ionization $\bar{Z}$. We know that many average ionizations can be calculated in the average-atom model [20,22]. In our case we have chosen to compute $\bar{Z}$ from the number of bound electrons ($\bar{Z}_B$), at the surface of the average-atom sphere ($\bar{Z}_R$), or from the continuum background ($\bar{Z}_{\text{CB}}$). We plot in Fig. 3 the pressure calculated using the three effective average ionizations compared to the AAM pressure. If we have an agreement at low temperature, we can see that the pressure calculated using $\bar{Z}_B$ progressively deviates from AAM. In this example, the pressures calculated using $\bar{Z}_R$ and $\bar{Z}_{\text{CB}}$ are very close to the AAM pressure. Yet, even if the $\bar{Z}_B$ pressure deviates from the AAM pressure, all the curves are inside the error bars of the QMD simulations. As a companion to this figure, we plot in Fig. 4 $(1-P_R/P_{\text{AAM}})$ and $(1-P_{\text{CB}}/P_{\text{AAM}})$ as a function of temperature where P_R, P_{CB}, and P_{AAM} are the pressures calculated using $\bar{Z}_R$, $\bar{Z}_{\text{CB}}$, and the average-atom model. We can see how close P_R and P_{CB} are from P_{AAM}. It could be interesting to have QMD pressure at 40 000 K with small error bars for comparison. In order to characterize the relativistic effects, we plot in Fig. 5 the nonrelativistic (NR) and the relativistic (Rel) pressures calculated using the average-atom model for gold at 0.5 g/cm^3. We can see that there is a small relativistic effect. Indeed, the electrons are more bound in the relativistic calculation. In this regime,

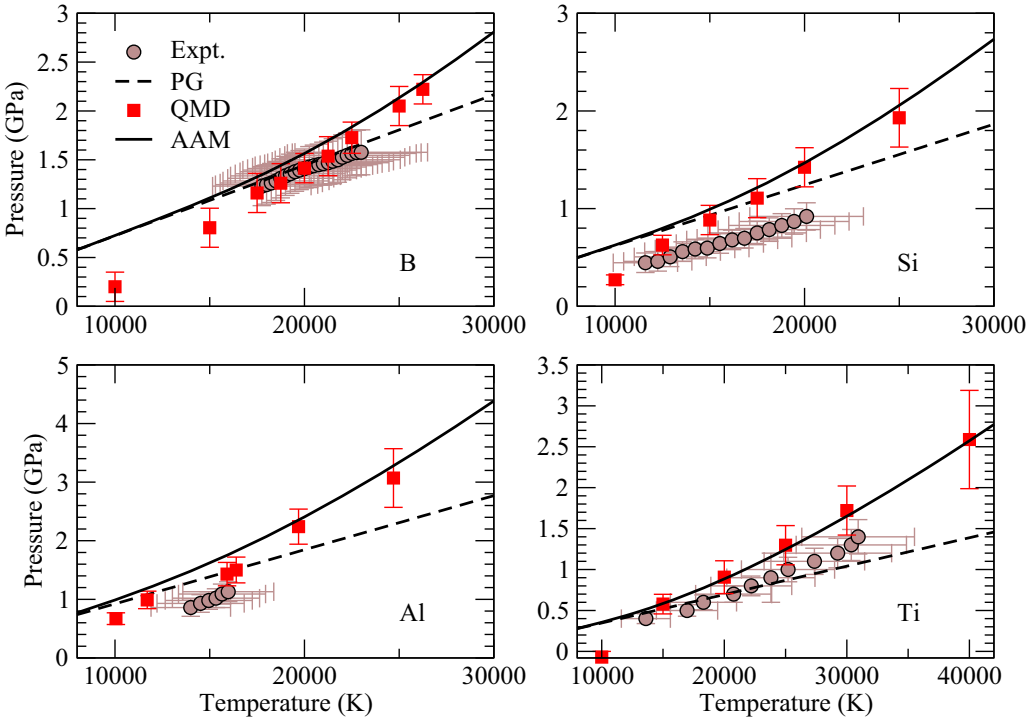

FIG. 1. Comparison of pressure between experiment (Expt.), the ion perfect gas (PG), QMD simulations (QMD), and the average-atom model (AAM) for boron at 0.094 g/cm^3, aluminum at 0.3 g/cm^3, silicon at 0.21 g/cm^3, and titanium at 0.2 g/cm^3.

the average ionization is smaller compared to the nonrelativistic calculation leading to a relativistic pressure P^{Rel} a little bit lower than the nonrelativistic pressure P^{NR}. We have the localization of orbital 7*s* in the relativistic calculation around 30 000 K due to the combined relativistic and temperature effects.

We now compare the pressure calculated using Eqs. (17) and (18) to QMD (DFT-MD) and PIMC simulations [5]

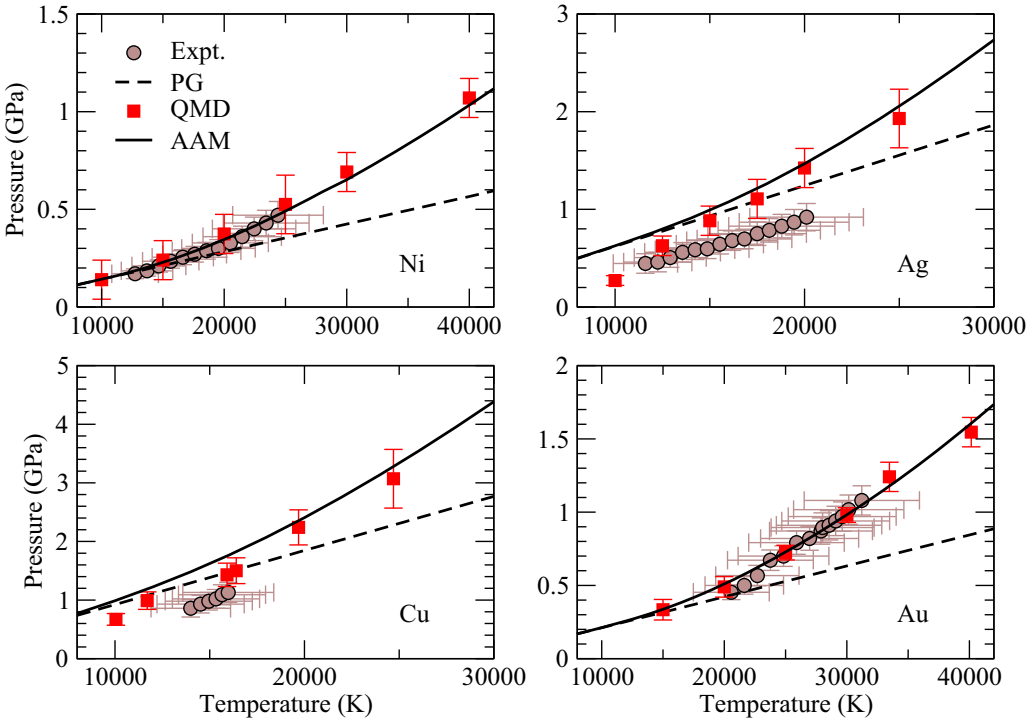

FIG. 2. Comparison of pressure between experiment (Expt.), the ion perfect gas (PG), QMD simulations (QMD), and the average-atom model (AAM) for nickel at 0.1 g/cm^3, copper at 0.5 g/cm^3, silver at 0.43 g/cm^3, and gold at 0.5 g/cm^3.

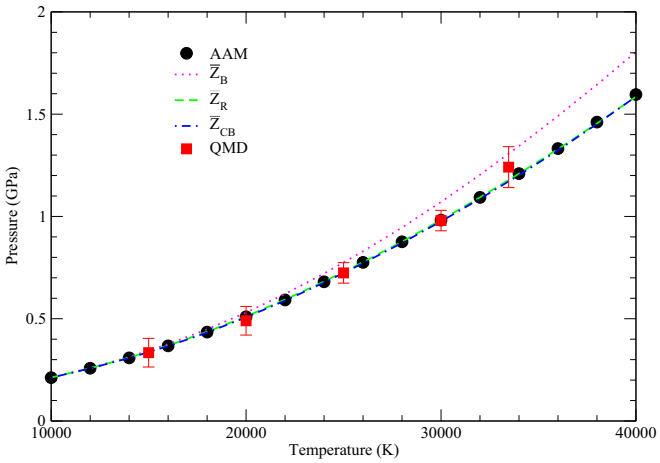

FIG. 3. Pressure calculated from the average-atom model (AAM) compared to three expressions using an effective average ionization for gold at 0.5 g/cm^3. $\bar{Z}_B$ is the average ionization obtained from the the number of bound electrons, $\bar{Z}_R$ from the electron density at the surface of the average-atom sphere, and $\bar{Z}_{\rm CB}$ from the continuum background. We give the QMD pressure (QMD) for the eyes.

for aluminum in the warm and hot dense matter in Fig. 6. The density is five times the solid density. We have a good agreement between DFT-MD/PIMC and AAM above 10 eV. The transition between QMD and PIMC is around 200 eV. There is a continuity between AAM and QMD/PIMC and between QMD and PIMC. The AAM deviates slightly from DFT-MD/PIMC simulations below 10 eV. At 10^4 K, the AAM approach gives a pressure of 35.90 Mbar whereas DFT-MD/PIMC simulations give 27.97 Mbar, leading to a relative error of 29%. In this regime, we are in the warm dense matter regime which is known to be difficult to describe with an average-atom model. In particular, the treatment of the ionic structure is too simple since we use the ideal gas approach. QMD is supposed to perform better in this regime.

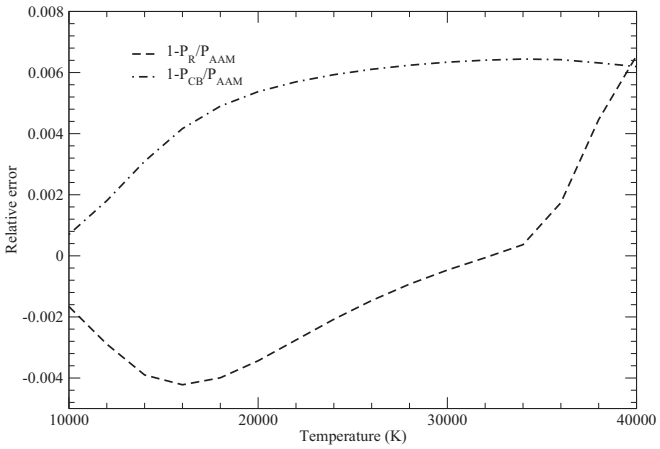

FIG. 4. Relative error of pressure calculated using $\bar{Z}_R$ and $\bar{Z}_{\rm CB}$ with respect to the average-atom model (AAM) for gold at 0.5 g/cm^3. $\bar{Z}_R$ is the average ionization obtained from the electron density at the surface of the average-atom sphere and $\bar{Z}_{\rm CB}$ from the continuum background.

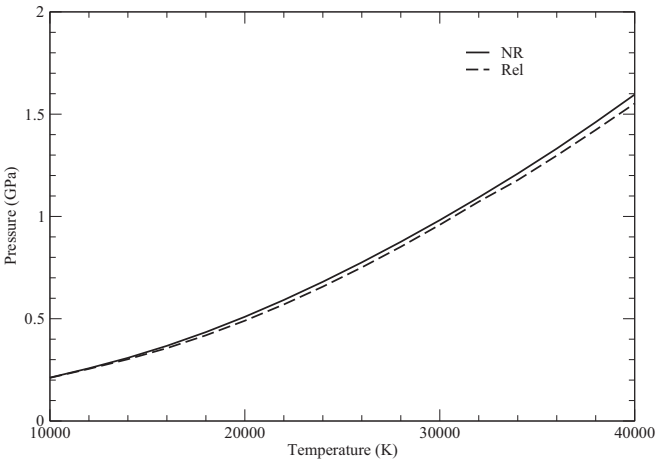

FIG. 5. Nonrelativistic (NR) and the relativistic (Rel) pressures calculated using the average-atom model for gold at 0.5 g/cm^3.

We plot in Fig. 7 the pressure as a function of compression for aluminum using DFT-MD simulations [5] and the AAM at 10^5 K. This temperature is supposed to be the temperature transition between the average-atom model and the QMD approach. Below this temperature, we use the QMD method and above we use the AAM. We can see that there is a relative error of the order of 10% between the two approaches.

IV. CONCLUSION

We have derived formulas to calculate the electronic pressure for the bound and continuum electrons using the stress tensor in the framework of the full-quantum average-atom model. Nonrelativistic and relativistic cases have been considered. There is a complete agreement between the nonrelativistic and relativistic formulas. We recover the nonrelativistic and relativistic free-electron gas pressures. Comparisons with QMD and PIMC simulations in the warm and hot dense matter regimes indicate that the present approach works well.

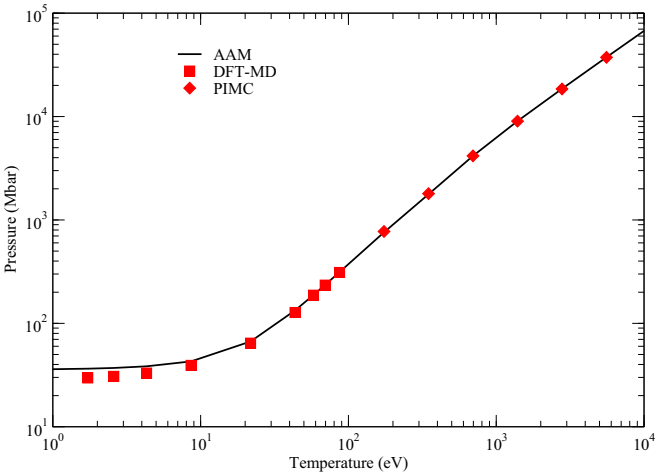

FIG. 6. Comparison of pressure between DFT-MD and PIMC simulations and the average-atom model (AAM) for aluminum at five times the solid density.

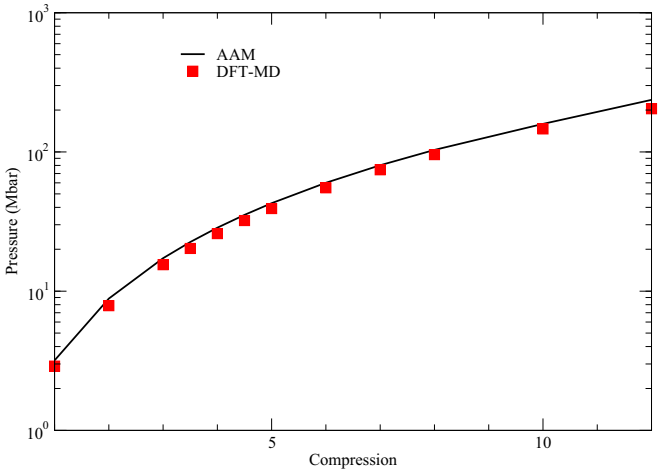

FIG. 7. Comparison of pressure between DFT-MD simulations (DFT-MD) and the average-atom model (AAM) for aluminum at 10^5 K as a function of compression.

Comparisons with experimental results in the warm dense matter regime are also satisfying.

APPENDIX: PROPERTIES OF THE SPHERICAL BESSEL FUNCTIONS OF THE FIRST KIND

The spherical Bessel function of the first kind $j_\ell(z)$ satisfies [43] the differential equation

$$z^2\frac{d^2 j_\ell(z)}{dz^2}+2z\frac{dj_\ell(z)}{dz}+[z^2-\ell(\ell+1)]j_\ell(z)=0, \quad \text{(A1)}$$

and the sum rule

$$\sum_\ell (2\ell+1)j_\ell^2(z)=1. \quad \text{(A2)}$$

In these expressions, ℓ is a positive integer running from 0 to $+\infty$. Let us differentiate Eq. (A2) with respect to z. We find that

$$\sum_\ell (2\ell+1)j_\ell(z)\frac{dj_\ell(z)}{dz}=0. \quad \text{(A3)}$$

Differentiating again, we find that

$$\sum_\ell (2\ell+1)\left(\frac{dj_\ell(z)}{dz}\right)^2=-\sum_\ell (2\ell+1)j_\ell(z)\frac{d^2 j_\ell(z)}{dz^2}. \quad \text{(A4)}$$

We now use successively the differential equation (A1), and the sum rules (A3) and (A2). We arrive at

$$\sum_\ell (2\ell+1)\left[\left(\frac{dj_\ell(z)}{dz}\right)^2+\frac{\ell(\ell+1)}{z^2}j_\ell^2(z)+j_\ell^2(z)\right]=2, \quad \text{(A5)}$$

or, we know that [15]

$$\sum_\ell (2\ell+1)\left(\frac{dj_\ell(z)}{dz}\right)^2=\frac{1}{3}. \quad \text{(A6)}$$

The proof of Eq. (A6) is as follows. We start from the identity [43,44]

$$e^{ix\cos\theta}=\sum_\ell (2\ell+1)i^\ell j_\ell(x)P_\ell(\cos\theta), \quad \text{(A7)}$$

where P_ℓ is the Legendre polynomial satisfying the orthogonality relation [43]

$$\int_{-1}^{1} dz P_\ell(z)P_{\ell'}(z)=\frac{2}{2\ell+1}\delta_{\ell\ell'}. \quad \text{(A8)}$$

We now differentiate Eq. (A7) with respect to x, multiply by its complex conjugate, and change $\cos\theta$ by z. We obtain

$$z^2=\sum_\ell\sum_{\ell'}(2\ell+1)(2\ell'+1)i^\ell(-i)^{\ell'}\frac{dj_\ell(x)}{dx}\frac{dj_{\ell'}(x)}{dx}P_\ell(z)P_{\ell'}(z). \quad \text{(A9)}$$

We then integrate this expression with respect to z between -1 and 1. Using the orthogonality relation (A8), we readily obtain Eq. (A6). Note that the sum rule (A2) can be obtained in a similar way from Eq. (A7) without differentiating with respect to x. Indeed, various sum rules can be derived by combining Eqs. (A7) and (A8). So, from Eqs. (A2), (A5), and (A6), we find the important identity

$$\sum_\ell \ell(\ell+1)(2\ell+1)j_\ell^2(z)=\frac{2z^2}{3}. \quad \text{(A10)}$$

[1] S. Atzeni and J. Meyer-ter-Vehn, *The Physics of Inertial Fusion: Beam Plasma Interaction, Hydrodynamics, Hot Dense Matter* (Clarendon, Oxford, UK, 2004).
[2] J. A. Gaffney *et al.*, High Energy Density Phys. **28**, 7 (2018).
[3] D. M. Ceperley, Rev. Mod. Phys. **67**, 279 (1995).
[4] L. Collins, I. Kwon, J. Kress, N. Troullier, and D. Lynch, Phys. Rev. E **52**, 6202 (1995).
[5] K. P. Driver, F. Soubiran, and B. Militzer, Phys. Rev. E **97**, 063207 (2018).
[6] S. X. Hu, B. Militzer, V. N. Goncharov, and S. Skupsky, Phys. Rev. Lett. **104**, 235003 (2010).
[7] S. X. Hu, B. Militzer, V. N. Goncharov, and S. Skupsky, Phys. Rev. B **84**, 224109 (2011).

[8] S. X. Hu, L. A. Collins, V. N. Goncharov, J. D. Kress, R. L. McCrory, and S. Skupsky, Phys. Rev. E **92**, 043104 (2015).
[9] S. X. Hu, R. Gao, Y. Ding, L. A. Collins, and J. D. Kress, Phys. Rev. E **95**, 043210 (2017).
[10] B. Militzer, Phys. Rev. B **79**, 155105 (2009).
[11] R. P. Feynman, N. Metropolis, and E. Teller, Phys. Rev. **75**, 1561 (1949).
[12] B. F. Rozsnyai, Phys. Rev. A **5**, 1137 (1972).
[13] D. A. Liberman, Phys. Rev. B **20**, 4981 (1979).
[14] S. J. Rose, J. Phys. B: At. Mol. Opt. Phys. **25**, 1667 (1992).
[15] T. Blenski and K. Ishikawa, Phys. Rev. E **51**, 4869 (1995).
[16] J. K. Yuan, Y. S. Sun, and S. T. Zheng, Phys. Rev. E **53**, 1059 (1996).
[17] B. Wilson, V. Sonnad, P. Sterne, and W. Isaacs, J. Quant. Spectrosc. Radiat. Transfer **99**, 658 (2006).
[18] W. R. Johnson, C. Guet, and G. F. Bertsch, J. Quant. Spectrosc. Radiat. Transfer **99**, 327 (2006).
[19] P. A. Sterne, S. B. Hansen, B. G. Wilson, and W. A. Isaacs, High Energy Density Phys. **3**, 278 (2007).
[20] M. S. Murillo, J. Weisheit, S. B. Hansen, and M. W. C. Dharma-wardana, Phys. Rev. E **87**, 063113 (2013).
[21] G. Faussurier, C. Blancard, P. Cossé, and P. Renaudin, Phys. Plasmas **17**, 052707 (2010).
[22] R. M. More, Adv. At. Mol. Phys. **21**, 305 (1985).
[23] N. Wetta, J.-C. Pain, and O. Heuzé, Phys. Rev. E **98**, 033205 (2018).
[24] W. Johnson, http://www3.nd.edu/~johnson/.
[25] W. Pauli, in *Handbuch der Physik*, Vol. 5 (Springer, Berlin, 1958), p. 1.
[26] J. S. Blakemore, Solid State Electron. **25**, 1067 (1982).
[27] M. Goano, Solid State Electron. **36**, 217 (1993).
[28] B. H. Bransden and C. J. Joachain, *Physics of Atoms and Molecules* (Longman Scientific & Technical, Harlow, 1992).
[29] W. R. Johnson, J. Nilsen, and K. T. Cheng, Phys. Rev. E **86**, 036410 (2012).
[30] G. Faussurier and C. Blancard, Phys. Rev. E **97**, 023206 (2018).
[31] H. Iyetomi and S. Ichimaru, Phys. Rev. A **34**, 433 (1986).
[32] J. J. Sakurai and J. Napolitano, *Modern Quantum Mechanics* (Pearson, New York, 2011).
[33] R. Parthasarathy, *Relativistic Quantum Mechanics* (Alpha Science, Oxford, UK, 2011).
[34] G. Faussurier, Phys. Plasmas **23**, 122704 (2016).
[35] A. Weiss, W. Hillebrandt, H. C. Thomas, and H. Ritter, *Cox and Giuli's Principles of Stellar Structure (Advances in Astronomy and Astrophysics)* (Cambridge Scientific Publishers, Cambridge, UK, 2006).
[36] Z. Gong, L. Zejda, W. Däppen, and J. M. Aparicio, Comput. Phys. Commun. **136**, 294 (2001).
[37] W. R. Johnson, *Atomic Structure Theory* (Springer, Berlin, 2007).
[38] Wolfram Research, Inc., Mathematica, Version 10.0, Champaign, IL, 2014.
[39] I. I. Sobelman, *Atomic Spectra and Radiative Transitions*, 2nd ed. (Springer, Berlin, 1992).
[40] R. Piron, Ph.D. thesis, Ecole Polytechnique, 2009.
[41] Y. K. Kim, Phys. Rev. **154**, 17 (1967).
[42] J. Clérouin, P. Noiret, P. Blottiau, V. Recoules, B. Siberchicot, P. Renaudin, C. Blancard, G. Faussurier, B. Holst, and C. E. Starrett, Phys. Plasmas **19**, 082702 (2012), and references therein.
[43] *Handbook of Mathematical Functions with Formulas, Graphs, and Mathematical Tables*, 9th ed., edited by M. Abramowitz and I. A. Stegun (Dover, New York, 1972).
[44] C. Cohen-Tannoudji, B. Diu, and F. Laloë, *Mécanique Quantique II* (Hermann, Paris, 1986).